Available online at www.sciencedirect.com
SCIENCE DIRECT®

Journal of the European Ceramic Society 24 (2004) 489–494

www.elsevier.com/locate/jeurceramsoc

# Toughening of NiAl–alumina composites by self-constructed compressive surface layers under oxidation

Osami Abe*, Satoshi Takata, Yoshitaka Ohwa

*The Research Center for Superplasticity, Faculty of Engineering, Ibaraki University, 4-12-1 Nakanarusawa, Hitachi 316-8511 Japan*

**Abstract**

Self-constructing protective layers have been fabricated on the surface of NiAl–alumina composites by the oxidation of NiAl to $NiAl_2O_4$. Dense NiAl–alumina materials for these tri-layer composites can be fabricated by a pressure-less sintering of the fine spherical powders derived from the chemically precipitated precursors. The sintered NiAl–alumina materials indicate high fracture toughness (5–6 $MPa.m^{1/2}$) suitable as the inner layer material sustained in the tensile stress against the compressive surface stress. The volume expansion under the oxidation of NiAl forming $NiAl_2O_4$ provides the compressive surface stress exhibiting the resistance to crack propagation. The determined compressive surface stress attaining to 128 MPa agrees with the estimation from the crack propagation, 170 MPa. The fracture toughness of the tri-layer materials containing fine-grained NiAl exceeds 8 $MPa{\cdot}m^{1/2}$. However, the excess oxidation for the 10 vol.%NiAl composition causes the formation of voids around the layer boundary to degrade the toughness with the relaxed residual stress.


*Keywords:* $Al_2O_3$; Composites; NiAl; Toughness and toughening

## 1. Introduction

Layered composites have attractive attributes for the toughening of ceramic materials.[1–6] One of the typical structure for layered materials is the multi-layer stacking of thin sheets in expectation of the extensive crack deflection along with the interfaces and the enhanced transformation toughening of tetragonal zirconia.[1–4] The other is the tri-layer structure consisting of strong outer layers with a flaw-tolerant inner layer.[5,6] For the tri-layer materials, in addition to the elastic mismatch, the thermal expansion mismatch of the layers is frequently applied to raise compressive surface stress during cooling from the sintering temperatures. This thermally induced compressive stress is a capable toughening mechanism, however, it should be disappear at elevated temperatures.

For the inner layer materials, ductile-phase-toughening using metallic constituents[7,8] is one of the most candidate possibilities. High-strength refractory intermetallics are potential materials as reinforcements for the inner layer materials sustained in the tensile response against the compressive stress in the outer layers. NiAl is one of the candidates because of its high melting point (1638 °C), high strength (1–2 GPa), and excellent oxidation resistance. The oxidation behavior forming $Ni_3Al$, Ni, $NiO + NiAl_2O_4$ consecutively suggested the possibility of strong binding of the dispersant/matrix interfaces providing the efficient ductile-phase bridging and the expanded plastic zone toughening.[9,10] It is also applicable for preparing self-constructive tri-layer composites with the compressive surface stress according to the following reaction (1).

$$\mathrm{NiAl}(5.89\ \mathrm{g\ cm^{-3}}) + 1/2\alpha\text{-}\mathrm{Al_2O_3}(\mathrm{matrix},\ 3.98\mathrm{g\ cm^{-3}}) = \mathrm{NiAl_2O_4}(4.51\ \mathrm{g\ cm^{-3}}) \quad (1)$$

The formation of low-density $NiAl_2O_4$ provides 8.2 and 16.4% expansion in volume for 5 and 10 vol.%NiAl/$\alpha$-$Al_2O_3$ composites after the complete oxidation. Strict binding of the layer interfaces due to the gradient boundary composition is also expected. The present paper deals with the preparation of NiAl/$\alpha$-$Al_2O_3$ composites through a chemically derived sinterable powder, the oxidation treatment providing tri-layer composites, and characterization of the layer interfaces.

* Corresponding author.
*E-mail address:* abe@hcs.ibaraki.ac.jp (O. Abe).

0955-2219/03/$ - see front matter © 2003 Elsevier Ltd. All rights reserved.
doi:10.1016/S0955-2219(03)00201-2

Table 1
Properties of sintered NiAl/α-$Al_2O_3$ composites

| | Sintering temperature $T_s$/°C | Density $\rho$/% | Grain size $d_{av}$/μm | Vickers hardness $H_v$/GPa | Fracture toughness $K_{IC}$/MPa $m^{1/2}$ | Residual stress $\sigma$R/MPa |
|---|---|---|---|---|---|---|
| α-$Al_2O_3$ | 1500 | 99.2 | $18.5_5$ | $16.7_9$ | $3.4_3$ | – |
| NiAl | 1460 | 96.7 | – | $4.9_1$ | – | – |
| NA05 | 1600 | 95.6 | $1.1_1$ | $14.8_9$ | $4.1_3$ | – |
| NA10a | 1500 | 97.1 | $1.0_2$ | $13.1_4$ | $5.9_0$ | – |
| NA10b | 1600 | 96.0 | $1.7_9$ | $14.6_5$ | $3.9_3$ | −30.4 |
| NA10c | 1550/1600[a] | 96.9 | $1.9_1$ | $11.6_7$ | $5.0_0$ | – |

[a] Two-step sintering at 1550 and 1600 °C.

## 2. Experimental

NiAl/α-$Al_2O_3$ composite powders (10 g) for the two compositions of 5 vol.%NiAl (NA05) and 10 vol.%-NiAl/α-$Al_2O_3$ (NA10) were prepared by a heat-treatment of mixtures of chemically precipitated (Ni,Al)-precursor and an α-$Al_2O_3$ powder (Taimei Chem., Co. Ltd., particle size: 100–150 nm). The precursor mixture for NA05 was prepared by pouring a methanol/water solution (100 $cm^3$) of $NiCl_2$ and $AlCl_3$ (1:1, every 8.43 mmol) into a precipitant solution (1.1 $dm^3$) dispersing the α-$Al_2O_3$ powder (9.278 g) at 50 °C. The precipitants were $C_6H_5COONH_4$ (84.3 mmol), $N_2H_5Cl$, (25.3 mmol), and $CH_3COONH_4$ (50.6 mmol as a buffer against HCl released from $N_2H_5Cl$). For NA10, the concentration of $NiCl_2$ and $AlCl_3$ increased to twice that of NA05 and 8.588 g α-$Al_2O_3$ powder was dispersed. The precipitate-to-reactant ratios were fixed. The determined composition of the precipitate was $[Ni(N_2H_4)_2Al](C_6H_5COO)_{3.7}(OH)_{1.3}$. The filtered and dried precursor mixtures were decomposed at 550 °C (2 h) and then reacted at 1250 °C (1.5 h) in a flowing Ar gas. The decomposition product was the fine mixture of the products (NiC, *am*-$Al_2O_3$, and free carbon) and *α*-$Al_2O_3$ dispersed. The α-$Al_2O_3$ with the comparatively large particle size hardly reacted at 1250 °C.[9] Residual carbon was removed by a heat-treatment at 600 °C in air. The obtained powders were pre-pressed to discs with the size of ϕ10×5 mm, CIP-ed at 150 MPa, and sintered at 1500–1600 °C for 2 h in Ar. The two flat surfaces of the sintered discs were ground by a 15 μm diamond wheel and polished to the thickness of 2.7 mm by using 1 μm diamond- and 0.1 μm $SiO_2$-abrasives. The surface oxidation was performed at 1300 °C (3 h), 1350 °C (3 h), 1400 °C (1, 3, 5 h) in air. The layer interface was characterized by an indentation test and SEM observation of the oxidation-derived material (1400 °C, 3 h) after removing certain amounts of the surface layers.

The sintered density was determined by Archimedes method. The crystalline phases were identified by X-ray diffractometry (XRD) using CuKα radiation (40 kV, 20 mA). The degree of oxidation ($\Psi$) of the surface NiAl was defined as $(1-I^N_{oxd}/I^N_{sint})V_f$, where $I^N_{sint}$ and $I^N_{oxd}$ were the integrated XRD intensity of NiAl (110) reflection for the sintered and oxidized materials, and $V_f$ was the volume fraction of NiAl. The Vickers hardness ($H_V$) and fracture toughness ($K_{IC}$, Evans equation) were determined by an indentation method at 196 N (20 s). The indent size and the crack length were measured by analyzing the SEM images at the magnification of ×150. The surface morphology was observed with

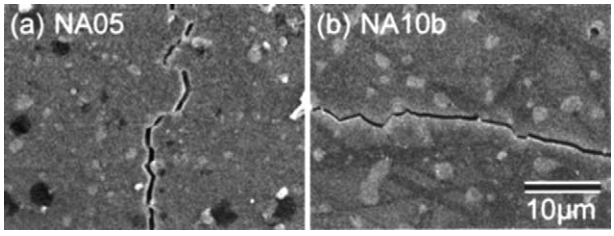


Fig. 1. Microstructure of sintered NiAl/α-$Al_2O_3$ composites.

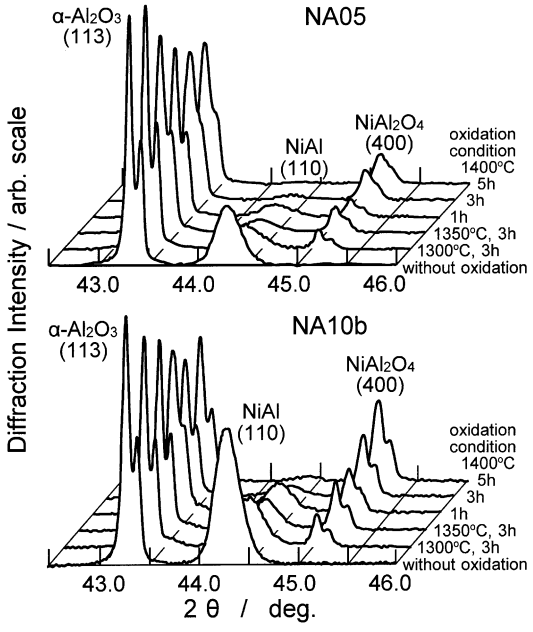


Fig. 2. X-ray diffraction profiles of the surface of oxidation-derived tri-layer composites.

SEM. The residual stress ($\sigma_R$) of the $\alpha$-$Al_2O_3$ matrix on the surface layers was determined by an X-ray method using FeK$\alpha$ radiation (40 kV, 36 mA, exposure: 600 s) with a $\phi$0.8mm collimator.

## 3. Results and discussion

The properties of sintered NiAl/$\alpha$-$Al_2O_3$ composites are listed in Table 1. High sintered density was obtained for the composites at the temperature of 1500–1600 °C. This good sinterability without an external pressure was provided by the morphology of the synthesized powders consisting of fine and spherical NiAl particles (<0.8 μm) covered with the finer $\alpha$-$Al_2O_3$ particles (0.1–0.2 μm).[10] The $H_V$ was a little smaller than that for $\alpha$-$Al_2O_3$. The thermal expansion mismatch between NiAl ($14.2\times10^{-6}$ $K^{-1}$, determined by dilatometry) and $\alpha$-$Al_2O_3$ ($10.9\times10^{-6}$ $K^{-1}$ at 1527 °C)[11] caused the compressive stress of −30.4 MPa (determined) for the $\alpha$-$Al_2O_3$ matrix in NA10b. This value agreed with the estimation (−25.4 MPa) by applying the following equation[6] to the crack propagation, meaning a certain contribution of the compressive stress as well as deflections and bridging.

$$K_{IC}^{obs} = \chi P c^{-3/2} + 2\,(c/\pi)^{1/2}\sigma_R^{calc} = \chi P (c')^{-3/2} \quad (2)$$

where $K_{IC}^{obs}$ is the fracture toughness, $P$ the applied pressure, $c'$ and $c$ the crack length of the composites and

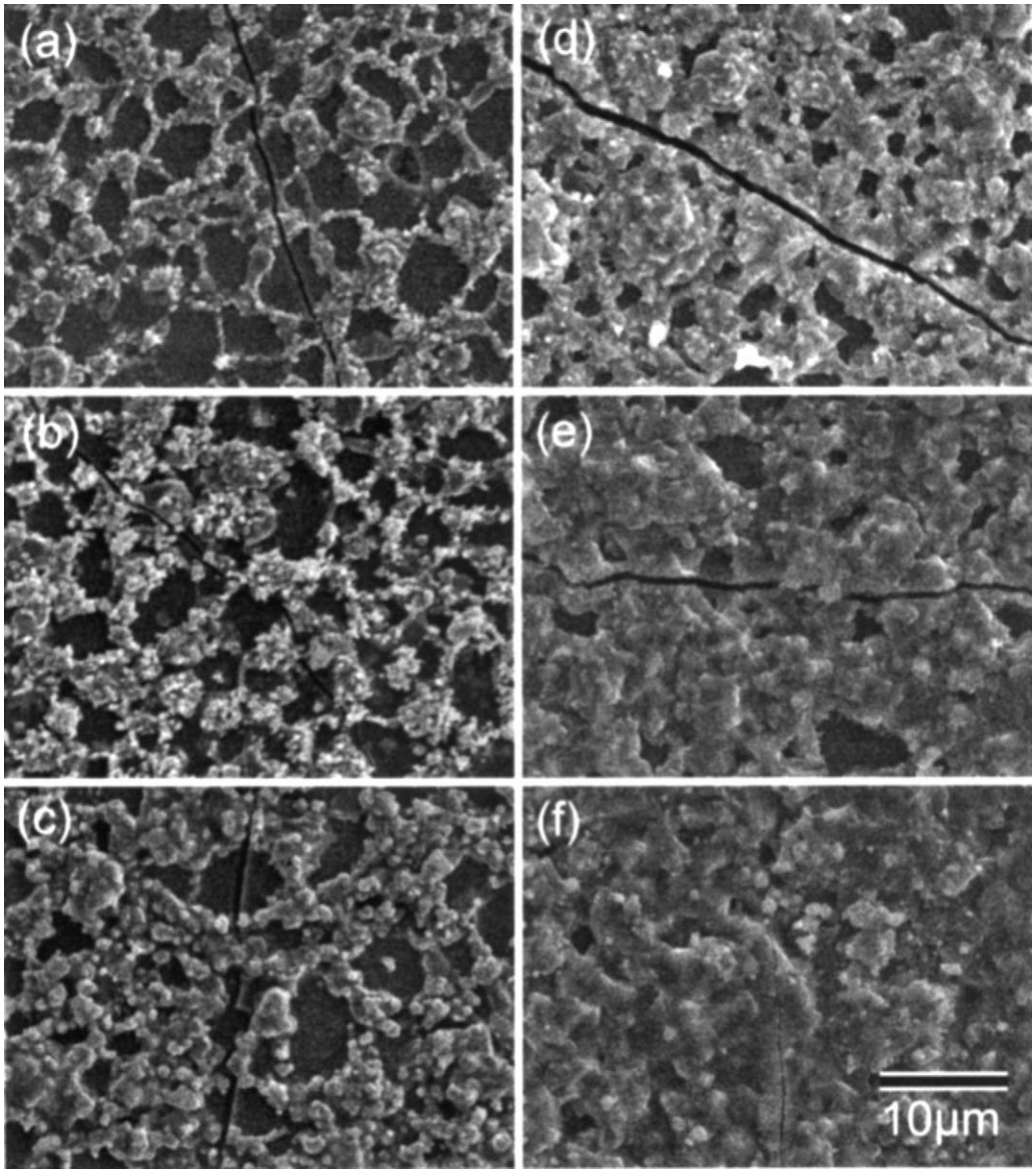


Fig. 3. Microstructure of the surface of oxidation-derived tri-layer composites: NA05 (oxidation 1300 °C, 3 h), $\Psi = 0.032$, (b) NA05 (1350 °C, 3h), $\Psi = 0.037$, (c) NA05 (1400 °C, 5 h), $\Psi = 0.048$, (d) NA10 (1300 °C, 3 h), $\Psi = 0.061$, (e) NA10 (1350 °C, 3 h), $\Psi = 0.070$, (f) NA10 (1400 °C, 5 h), $\Psi = 0.091$.

the monolithic matrix phase, $\sigma_R^{calc}$ the residual stress, and $\chi$ a constant. The $K_{IC}^{obs}$ was improved by the addition of NiAl. However, for the NA10 composition, the observed $K_{IC}^{obs}$ values were dispersed depending on the sintering condition. One of the reasons for the difference in $K_{IC}^{obs}$ is the size of dispersant NiAl (Table 1), which influences not only the ductile-phase bridging and plastic zone toughening but also on the contribution of compressive stresses.

The typical microstructure of the sintered composites is shown in Fig. 1. The ductile bridging around the NiAl grains was evident for NA05 with a smaller grain size. Then, the dispersion of small NiAl grains is efficient for toughening. The reason for the increased $K_{IC}^{obs}$ for NA10c with larger grains was unclear, but the enhanced deflection was observed. The composites NA05, NA10a and NA10b were used to prepare oxidation-derived trilayer composites. The other material, NA10c, was used for the characterization of the layer boundary by removing the surface layer after oxidation at 1400 °C for 3 h.

The surface NiAl grains were oxidized by the heat-treatment as shown in Fig. 2. The diffraction intensity for NiAl decreased and, contrary, that for $NiAl_2O_4$ increased with the progress in oxidation. No reflections for NiO were observed despite the fact it was detected as an oxidation product of the NiAl powders.[10] This suggested the reaction of NiO with the matrix $\alpha$-$Al_2O_3$, perhaps at the grain boundary with poor crystallinity, to form $NiAl_2O_4$. The degraded separation of the $K\alpha_1$ and $K\alpha_2$ reflections for $\alpha$-$Al_2O_3$ at 1400 °C suggested the generation of stresses inside the grains.

To examine the two possibilities from the XRD profiles, SEM observation and the determination of residual stress have been performed. Fig. 3 shows the surface morphology of the oxidized composites. The surface of the composites was covered with the

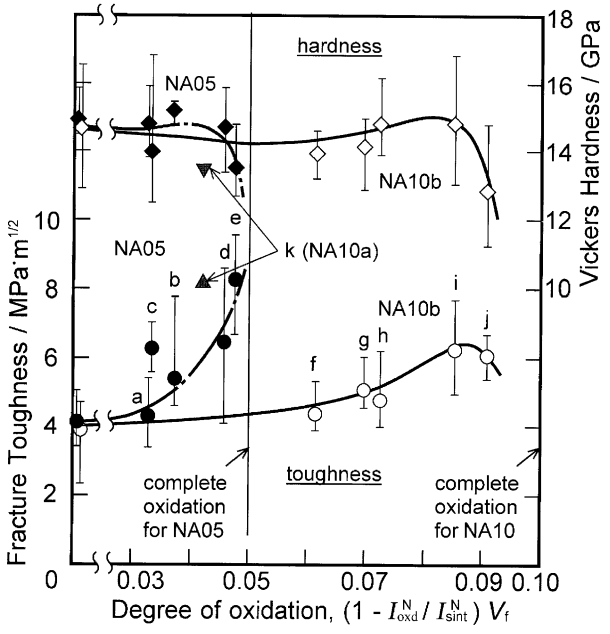


Fig. 4. Vickers hardness and fracture toughness of the oxidation-dereived trilayer composites as functions of the degree of oxidation: (a, f) oxidation 1300 °C, 3 h, (b, g) 1350 °C, 3 h, (c, h) 1400 °C, 1 h, (d, i) 1400 °C, 3 h, (e, j) 1400 °C, 5 h, (k) NA10a (1 μm NiAl, 1300 °C, 0.5 h).

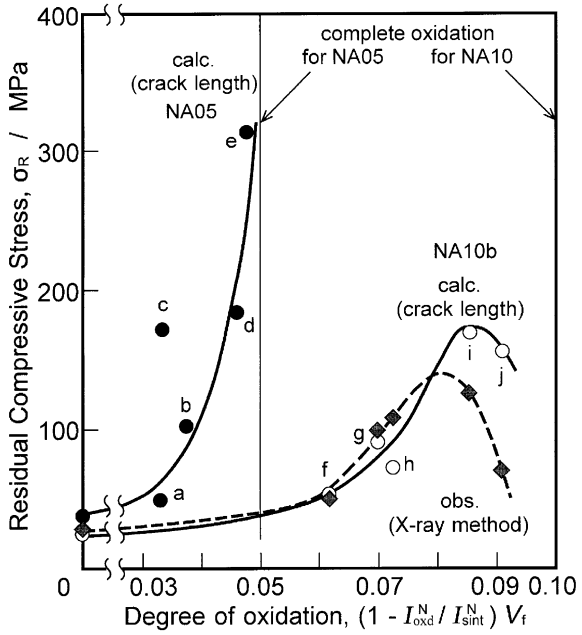


Fig. 5. Determined and estimated compressive stress in the surface layers: (a, f) oxidation 1300 °C, 3 h, (b, g) 1350 °C, 3 h, (c, h) 1400 °C, 1 h, (d, i) 1400 °C, 3 h, (e, j) 1400 °C, 5 h.

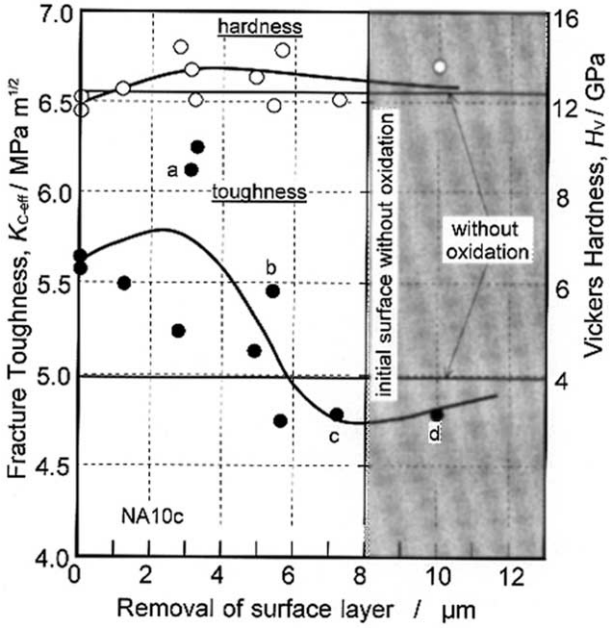


Fig. 6. Influence of surface removal on Vickers hardness and fracture toughness of the oxidation-derived tri-layer composite NA10c.

networks of $NiAl_2O_4$, meaning the boundary diffusion of $Ni^{2+}$ forming $NiAl_2O_4$. The network structure was much developed with the increase in oxidation temperature, the prolonged oxidation time, and the increase in NiAl content. Straight transgranular cracks were observed after the oxidation treatment, while the cracks for the as-sintered NiAl/α-$Al_2O_3$ composites deflected markedly. Figs. 4 and 5 show the $H_V$ and $K_{IC}^{obs}$ of the oxidation-derived tri-layer composites and the residual compressive stress ($-\sigma_R$), as functions of the degree of oxidation, $\Psi=(1-I_{oxd}^{N}/I_{sint}^{N})V_f$, The complete oxidation of NiAl for NA05 and NA10 corresponds to 0.05 and 0.10 in $\Psi$, respectively. The improvement of the $K_{IC}^{obs}$ and the good agreement of the determined compressive stress ($-\sigma_R^{obs}$) with that of the estimation ($-\sigma_R^{calc}$) from Eq. (2) were observed for NA10b at $\Psi<0.085$. This meant the dominant contribution of the oxidation-derived compressive stress to toughening for NA10b. However, the $K_{IC}^{obs}$ for NA05 did not improved at $\Psi=0.033$, where the volume expansion was estimated as 7.9% according to the reaction (1). A certain fraction of the volume expansion should be consumed to fill the residual pores of the sintered composites ($\rho=95.6\%$). The growth of the oxidation product vertical to the surface was also unavailable to toughening. In addition, it was supposed that the continuous network formation was required for the improvement of fracture toughness. The weak connection among the partly developed networks would not contribute to toughening. When the strict network was developed, as shown in Fig. 3b and c, the toughness increased markedly. For NA10b, $K_{IC}^{obs}$ was not improved up to 0.012 in $\Psi$, although the network evidently developed on the surface at 1300 °C. It increased to $6.3_3$ MPa $m^{1/2}$ after oxidation for 5 h at 1400 °C ($\Psi=0.085$, $\sigma_R^{obs}=-128$ MPa). It was considered that this delayed improvement for NA10b was due to the large size of the NiAl grains, because the other material, NA10a, with the finer size of NiAl grains indicated the high fracture toughness of $8.1_4$ MPa $m^{1/2}$ at $\Psi=0.042$.

For tri-layer composites, $\sigma_R$ due to the linear expansion, $\Delta\varepsilon$, is estimated by the following equation.[6] NA10b with $\Psi=0.08$.

$$\sigma_R = -\Delta\varepsilon E\delta[(1-\nu)d]^{-1} \quad (3)$$

where $E$ is the Elastic modulus (367 GPa), $\delta$ and $d$ the thickness of the surface layer and specimen, $\nu$ the Poisson's ratio (0.25). When assuming the effective linear expansion, $\Delta\varepsilon_{eff}=[1+\Delta V-(1-\rho)]^{1/3}-1$, after filling the residual pores in non-oxidized NiAl/α-$Al_2O_3$ composites and $\delta=20\times10^{-6}$ m as the delaminating depth observed at a high applying load (294 N), the $\Delta V$ obtained according to Eq. (1) for NA10b ($\Psi=0.085$) provides the calculated $\sigma_R$ of −146 MPa. This value shows the good agreement with the determined $-\sigma_R^{obs}$ (−128 MPa) and the estimation from crack propagation (−170 MPa). However, the calculation for NA05

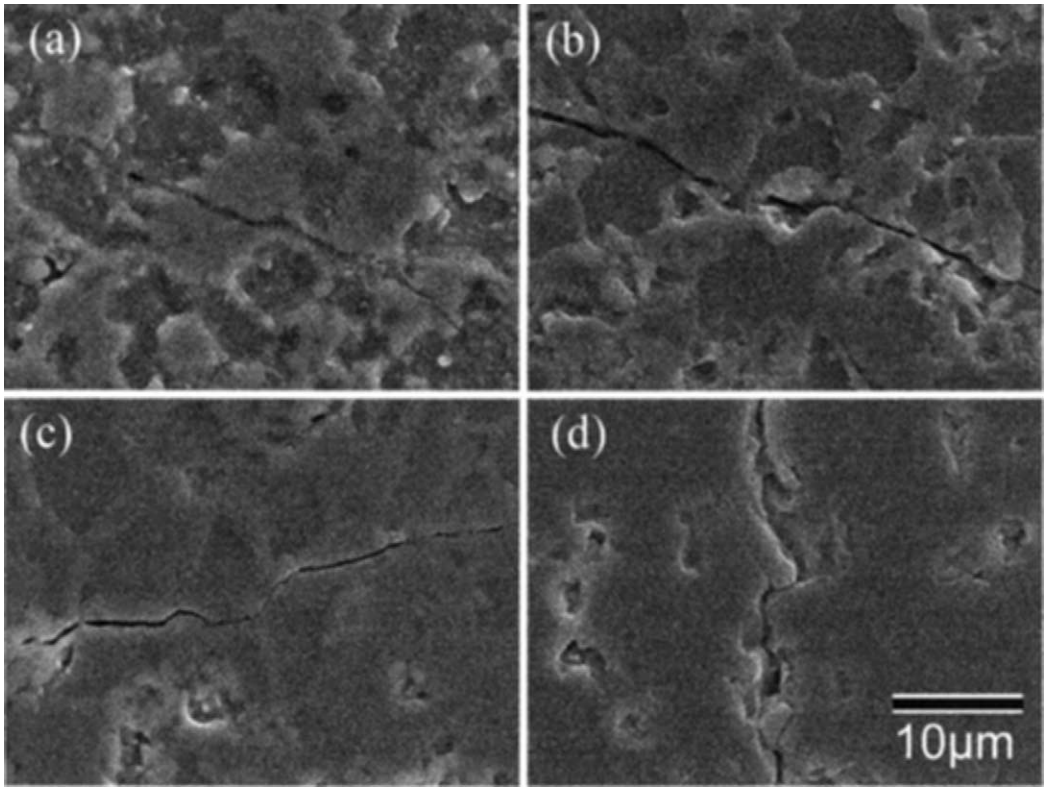


Fig. 7. Microstructure of the surfaces with (a) 3.2 μm, (b) 5.3 μm. (c) 7.2 μm, and (d) 10.0 μm removal.

($\sigma_R = -60$ MPa at $\Psi = 0.05$) is evidently smaller than the estimation from the crack length. The difference would be ascribed by the assumption of $\delta$, neglected difference in $E$ between the surface and inner layers in Eq. (3),[6] and the influence of deflection of the cracks inside the layers and along with the layer interface.

Another observation from Figs. 4 and 5 was the degradation of $H_V$, $K_{IC}^{obs}$ and $\sigma_R^{obs}$ at $\Psi = 0.091$ for NA10b. The property degradation accompanying with the reduced compressive stress supposed the formation of defects at the layer boundary. Then, the influence of the removal of the surface layer on $K_{IC}^{obs}$ was examined for the oxidized NA10c. Fig. 6 indicated the $H_V$ and $K_{IC}^{obs}$ as functions of the surface removal. Although the smaller removal than the depth of the indent (about 20 μm), the measured values must reflect the properties of the surface layer removed. The removal of 6–10 μm surface layer resulted in the smaller $K_{IC}^{obs}$ than that of the non-oxidized material. It is considered that the very thin surface layer less than 5 μm makes an important contribution to toughening. The microstructure of the removed surfaces is represented in Fig. 7. Almost straight cracks with reduced crack opening were observed for the materials with the removal of 3.2 and 5.3 μm (Fig. 7a and b). The boundary propagation of the cracks was dominant around the initial surface without oxidation (c). The formation of $NiAl_2O_4$ with less resistivity to crack propagation would enhance the deflection as observed in Fig. 7c. When removing to 2 μm inside the initial surface (d), many voids were observed. It is considered that these voids are generated by the diffusion of nickel along with the grain boundary.

## 4. Conclusions

The fabrication and characteristics of NiAl/α-$Al_2O_3$ composites and the derived tri-layer composites with self-constructed compressive surface layers under oxidation have been described. The dispersion of the intermetallic NiAl into the α-$Al_2O_3$ matrix is efficient to form a stress-tolerant material suitable to the inner layer for the tri-layer composites. The volume expansion due to the oxidation of NiAl forming $NiAl_2O_4$ at 1300–1400 °C provided the surface layers with the residual compressive stress. The fracture toughness of the obtained tri-layer composite is improved to 8 MPa $m^{1/2}$ for 5 vol.%NiAl and 10 vol.%NiAl compositions with fine NiAl grains. Chemical reaction is available to form protective layers alternatively to the use of thermal expansion mismatch.

## Acknowledgements

This work has been conducted under the financial support of Grant-in-Aid for Scientific Research (B), The Ministry of Science and Education, Japan (No.13450275). The authors wish to provide sincere thanks for the assistance.

## References

1. Clegg, W. J., Kendall, K., Alford, N. M., Button, T. W. and Birchall, J. D., A simple way to make tough ceramics. *Nature (London)*, 1990, **347**, 455–457.
2. Marshall, D. B., Ratto, J. J. and Lange, F. F., Enhanced fracture toughness in layered microcomposites of Ce–$ZrO_2$. *J. Am. Ceram. Soc.*, 1991, **74**, 2979–2987.
3. Abe, O. and Yamada, J., Preparation of multi-layer composites by combination of centrifugal filter pressing and rate-controlled sintering. *J. Ceram. Soc. Japan*, 1994, **102**, 627–632.
4. Kuo, D. and Kriven, W. M., A strong and damage-tolerant oxide laminate. *J. Am. Ceram. Soc.*, 1997, **80**, 2421–2424.
5. Virker, A. V., Jue, J. F., Hansen, J. J. and Cutler, R. A., Measurement of residual stress in oxide-$ZrO_2$ three layer composites. *J. Am. Ceram. Soc.*, 1988, **71**, C–148-C-151.
6. Sathyamoorthy, R., Virker, A. V. and Cutler, R. A., Damage-resistant SiC–AlN layered composites with surface compressive stresses. *J. Am. Ceram. Soc.*, 1992, **75**, 1136–1141.
7. Chen, Z. and Mecholsky, J. J., Toughening by metallic lamina in nickel/alumina composites. *J. Am. Ceram. Soc.*, 1993, **76**, 1258–1264.
8. Fahrenholtz, W. G., Ellerby, D. T. and Loehman, R. E., $Al_2O_3$–Ni compacts with high strength and fracture toughness. *J. Am. Ceram. Soc.*, 2000, **83**, 1279–1280.
9. Abe, O. and Takata, S., Preparation of NiAl/$Al_2O_3$ composites. *Key Engineering Materials*, 1999, **159–160**, 319–324.
10. Abe, O. Intelligent alumina–NiAl material having sensitivity to oxidation damages. In *Proc. 6th Japan International SAMPE Symposium*, ed. Tanimoto, T., Morii, T. Japan Chapter of SAMPE, Tokyo, pp. 237–240, 1999.
11. Thermophys. Properties of Mater., The TPRC Data Series, Vol.13, *Thermal Expansion of Nonmetallic Solids*. p.176, 1977.